Modelling the high-resolution dynamic exposure to flood in city-region

Xuehong Zhu[1], Qiang Dai[1, 2, *], Dawei Han[2], Lu Zhuo[2], Shaonan Zhu[3], Shuliang Zhang[1, *]

[1]Key Laboratory of VGE of Ministry of Education, Nanjing Normal University, Nanjing, China
[2]WEMRC, Department of Civil Engineering, University of Bristol, Bristol, UK
[3]College of Geographical and Biological Information, Nanjing University of Posts and Telecommunications, Nanjing, China
*Correspondence: q.dai@bristol.ac.uk

Abstract:

Urban flooding exposure is generally investigated with the assumption of stationary disasters and disaster-bearing bodies within an event, and thus cannot satisfy the increasingly elaborative modelling and management of urban flood. In this study, a comprehensive method was developed to simulate dynamic exposure to urban flooding considering residents' travel behavior. First, a flood simulation was conducted using the LISFLOOD-FP model to predict the spatio-temporal distribution of flooding. Second, an agent-based model was used to simulate residents' movements during the period of urban flooding. Finally, to study the evolution and patterns of urban flooding exposure, the exposure of population, roads, and buildings to urban flooding was simulated using Lishui, China as the case study. The results indicated evident spatio-temporal variations in urban flooding and population distribution. Additionally, the exposure increased with increasing rainfall and flooding severity. The urban area near the Oujiang River was the most severely flooded and indicated the largest amount of exposure of population, roads, and buildings. Furthermore, the impacts of flooding on roads were greater than those on population and on buildings. This study presents the first fully formulated method for dynamic urban flood exposure simulation at high spatio-temporal resolution. The results of this study can provide baseline data for determining urban flood disaster vulnerability, socioeconomic loss assessment, urban disaster risk management, and for establishing emergency response plans.

Keywords: urban flooding; resident travel behavior; agent-based model; dynamic exposure

1. Introduction

Storm flooding has become increasingly frequent and severe with the intensification of global warming and the rising frequency of extreme weather events (*Dankers and Feyen, 2008*; *Hammond et al., 2015*). Urban floods have become major natural disasters in many cities around the world and have created serious threats to human life and social and economic activities (*Gain et al., 2015*). Effectively coping with floods and their adverse effects is an important part of disaster prevention and mitigation as well as disaster risk management (*Atta-Ur-Rahman, 2014*). Non-engineering measures such as exposure assessment are currently the main way of managing urban flooding risk (*Chen et al., 2015*). Exposure refers to the presence of people, livelihoods, environmental services and resources, infrastructure, or economic, social, or cultural assets in places that could be adversely affected by natural disasters (*IPCC, 2012*). Urban flood disasters are caused by the adverse effects of heavy rain and other factors on the city system in certain disaster-prone ~~pregnant~~ environments. These events consist of three parts: the disaster-causing factors, the disaster-pregnant environment, and the disaster-bearing bodies (*Shi, 1996*).

Exposure has obvious dynamic characteristics because of the dynamic evolution of urban floods and disaster-bearing bodies. Therefore, the characteristics of flood disasters and building environments and the distribution of population and socio-economic resources are the key factors for evaluating urban flood exposure. The methods for evaluating exposure to urban flooding at a certain time or period vary due to changes in the disaster-bearing bodies, study areas, data acquisition methods, etc. (*Röthlisberger et al., 2017*). Index-based methods are commonly used for comprehensive exposure evaluation (*Mahe et al., 2005*; *Mansur et al., 2016*; *Guo et al., 2014*).

The exposure index method is to select the natural, social, economic and other evaluation indexes from the characteristics of the disaster-bearing bodies to establish the evaluation index system, determine the index weights by the analytic hierarchy process and expert scoring method, construct the evaluation system by using mathematical model, and obtain the exposures of the disaster-bearing bodies (*Nasiri et al., 2016*). Statistical methods based on historical disaster data are also utilized (*Moel et al., 2011*).

With respect to spatial considerations, the currently implemented method for estimation of disaster exposure adopts the administrative boundaries of socioeconomic data, which are organized as research units (*Yin, 2009*). Consequently, natural elements that have higher spatial resolutions must be compromised due to the lower spatial resolution of human elements like population (*Yang et al., 2013*). Therefore, a comprehensive and sophisticated geographic research unit has not been established, thus resulting in simulation results applicable only to macro planning and decision making. Hence, the estimation of disaster exposure needs to incorporate greater spatial heterogeneity and resolution.

Besides enhancement of the spatial scale, dynamic temporal simulation of disaster exposure has gained increasing attention. Specifically, the dynamic evolution of disaster exposure at the macro time scale considers exposure distribution as well as its variation during different development periods (*Weis et al., 2016*). Therefore, this method is relatively mature and has led to abundant research results. At the micro time scale, disaster-causing factors and disaster-bearing bodies represented by populations are constantly varying. On the one hand, spatio-temporal changes in disaster-causing factors (rainfall) result in corresponding dynamic changes in the characteristics (water depth and velocity) of urban flood disasters. On the other hand, daily travel activities of urban residents, such as commuting between residential and work or learning spaces, cause a dynamic spatio-temporal distribution of the population. At the same time, the exposure to urban flooding changes dramatically over a short period of time. To avoid or reduce disaster risks, casualties, and property losses, different individuals are likely to adopt different adaptive behaviors, such as delaying or cancelling travel plans, while the government is likely to adopt organizational actions such as issuing warnings and evacuating residents (*Wan and Wang, 2017*; *Parker et al., 1995*). Thus, the dynamic simulation of exposure requires the dynamic space-time simulation of variations in the disaster, disaster-bearing bodies, as well as interactions between them. Modeling of the temporal and spatial changes in natural disasters mainly uses the disaster system simulation method, and the typical representative used is a hydrological or hydrodynamic model to simulate flood disasters (*Werren et al., 2016*). The change simulation of the disaster-bearing body (population) can use the method based on individual space-time mark data (*Liang et al., 2015*) and the agent-based method (*Kang et al., 2012*). Although the former can acquire the human position and moving track, it is difficult to identify the purpose of human activities, and human disaster response behavior cannot be simulated. The agent-based model (ABM) can not only simulate the population distribution but can also simulate the interaction among the population (as the disaster victim), the hazard factors, and the disaster-pregnant environment (*Yin, et al., 2016b*). Current research has used the ABM to simulate human responses to disasters, which, in turn, have been used in natural disaster risk research (*Johnstone, 2012*; *Huang et al., 2015*). Nevertheless, the simulation results do not reflect the exposure characteristics of the disaster-bearing bodies and their dynamic changes (*Dawson et al., 2011*).

Therefore, the objectives of this study were to develop a novel method using the LISFLOOD-FP model (Sect. 3.1) and an ABM (Sect. 3.2) to simulate the exposure of urban populations, roads, and buildings to flooding under varying conditions and subsequently implement the method as a pilot study in a real city. Several scenarios, including diverse flooding types and various responses of residents to flooding, were considered in this regard. Additionally, dynamic features of the real world were incorporated to improve the micro exposure analysis. This method was subsequently applied to an urban area as a case study. Exposure simulation is a useful tool for estimation of disaster vulnerability and assessment of losses, and the results of this study are likely to benefit the relevant government agencies in assessing risk, issuing warnings, and planning emergency responses to urban natural disasters.

2. Study area and data source

In this study, Lishui City in Zhejiang Province, China, was considered as the study region because of the availability of the required data and flooding history. The urban district of Lishui is a largely hilly and mountainous area, and the Oujiang River traverses its southern and eastern parts. The study area is located in the central district of Lishui, covers an area of 43.4 km^2, and has a large population of about 71673 (Fig. 1). The frequencies of heavy rainstorms and persistent concentrated rainfall events rise sharply in May and June during the Meiyu flood period, which often results in flood disasters. On August 20, 2014, a heavy rainfall event lasting a few days produced a 50-year flood in Lishui and caused considerable loss of property.

The datasets used in this study included a digital elevation model and data for rivers, roads, buildings, population, and observation data consisting of flow and water level. Traffic flow and water accumulation data were used for validation. Table 1 describes the sources and uses of the datasets.

Survey data was used to generate daily routine. There were 500 residents participated in the survey. Among them, there were 100 people under 18 years old, 300 middle-aged people and 100 elderly people. Employed people and male people accounted for 55% and 50%, respectively. And 14% of the population had received higher education. The distribution of the above social characteristics is close to the actual population distribution in the study area.

3. Methodology

This study comprised three aspects: disaster simulation, human activity simulation, and dynamic exposure assessment (Fig. 2). The first step included fluvial and pluvial flooding simulation based on the LISFLOOD-FP model. The simulation of human activity utilized ABM to obtain the spatio-temporal distribution of the population under different scenarios. Finally, the developed model was combined with the results of the previous two steps to assess the dynamic exposure of the population, roads, and buildings to urban flooding.

3.1 Flood models

A wide variety of existing hydrological or hydrodynamic models are available that are capable of simulating fluvial or pluvial flooding, including the Storm Water Management Model (SWMM) (*Rossman, 2015*), LISFLOOD (*Bates and De Roo, 2000*), MIKE-SHE (*DHI, 2000*), MIKE-11 (*Havnø et al., 1995*), MOUSE (*Lindberg et al., 1989*), HEC-RAS (*Brunner, 2008*), and HEC-HMS (*Charley et al., 1995*). LISFLOOD-FP (*Bates et al., 2013*) is a coupled 1D/2D hydraulic model based on a raster grid and was designed for research purposes at the University of Bristol. LISFLOOD-FP uses a square grid as the computational grid to simulate one-dimensional river hydraulic changes and two-dimensional floodplain hydraulic changes. The applicability of the model has been verified by several studies (*Horritt and Bates, 2002*; *Bates and De Roo, 2000*). Therefore, the LISFLOOD-FP model was chosen for the simulation of fluvial and pluvial flooding.

Floodplain flows were described in terms of the continuity and momentum equations discretized over a grid of square cells, which allowed the model to represent 2D dynamic flow fields for the floodplain. It assumed that the flow between two cells was simply a function of the free surface height difference between those cells:

$$\frac{dh^{i,j}}{dt} = \frac{Q_x^{i-1,j} - Q_x^{i,j} + Q_y^{i,j-1} - Q_y^{i,j}}{\Delta x \Delta y}, \tag{1}$$

$$Q_x^{i,j} = \frac{h_{flow}^{5/3}}{n} \left(\frac{h^{i-1,j} - h^{i,j}}{\Delta x} \right)^{1/2} \Delta y, \tag{2}$$

where $h^{i,j}$ is the free surface height of water at node (i,j), Δx and Δy are the cell dimensions, n is the effective grid scale Manning's friction coefficient for the floodplain, and Q_x and Q_y describe the volumetric flow rates between the floodplain cells. Q_y is defined analogously to Q_x.The flow depth, h_{flow}, represents the depth through which water can flow between two cells, and d is defined as the difference between the highest free surface height of water in the two cells and the highest bed elevation.

The types of flooding simulated in this study included pluvial and fluvial floods. Synthetic rainfall data for a return period of 50 years used for pluvial flood simulation were simulated using the Chicago hyetograph method (CHM) (*Cen et al., 1998*). The rainfall data were determined using the rainstorm intensity formula (Eq. (3)), rainfall duration time (T), and peak position (r).

$$i = \frac{A(1 + c \log P)}{167(t+b)^n}, \tag{3}$$

where i is the rainfall intensity (mm/min), P is the return period, and t is the time. A, b, c and n are parameters related to the characteristics of the local rainstorm and need solutions. A is the rainfall parameter, i.e. the design rainfall (mm) for 1 min at a 10 year return period, c is the rainfall variation parameter (dimensionless), and b is the rainfall duration correction parameter, i.e. the time constant (min) that can be added to convert the curve into a straight line after logarithmic calculation of the two sides of the rainstorm intensity formula. n is the rainstorm attenuation index, which is related to the return period. The rainfall duration was 6 hours (6 am to 12 pm), and the accumulated rainfall was nearly 148 mm. The "r" refers to the relative rainfall peak time, i.e., the value from zero to one. Zero means the maximum rainfall at the beginning of rainfall and one means the maximum rainfall at the end of rainfall. Here, we fixed r at 0.2 based on the assumption that the peak is located at the one fifth point of the design hyetograph. The parameters A, b, c and n were estimated from the rainstorm intensity formula for Lishui City obtained from the "Zhejiang City Rainstorm Intensity Formula Table" published by the Hangzhou Municipal Planning Bureau (Table 2). The rainfall simulation results are shown in Fig. 3(a). The flow and water level input data for fluvial flood simulation utilized observational data from Lishui's 50-year flood in 2014, provided by the Liandu Hydrological Station (Fig. 3(b)). The flow data for the Daxi and Haoxi rivers on August 20, 2014 were obtained from the Xiaobaiyan and Huangdu stations, respectively, and the observational data for water levels at the outlets were those for the Kaitan Dam.

3.2 ABM

Several modeling techniques, often collectively referred to as social simulation, have been successfully used to represent the behaviors of humans and organizations. These include event and fault trees, Bayesian networks, microsimulation, cellular automata, system dynamics, and ABMs. Research methods based on ABMs have been gradually introduced to the field of natural disaster risk assessment. ABM is considered most suitable to address challenges associated with simulating the complexity and dynamic variability of population exposure to flooding due to its capacity to capture interactions and dynamic responses in a spatial environment (*Dawson et al., 2011*).~~.~~

An ABM is a computational method for simulating the actions and interactions of autonomous decision-making entities in a network or a system to subsequently assess their effects on the system as a whole. Individuals and organizations represent agents. Each agent individually assesses its situation and makes decisions based on a set of rules. Agents may execute various behaviors appropriate for the system component they represent—for example, producing or consuming. Therefore, an ABM consists of a system of agents and the relationships between them. Even a simple ABM can exhibit complex behavior patterns because a series of simple interactions between individuals may result in more complex system-scale outcomes that could not have been predicted just by aggregating individual agent behaviors.

The ABM was developed as a concept in the late 1940s, and substantial applications were realized with the emergence of high-powered computing. Such applications include those in the political sciences (*Axelrod, 1997*), management and organizational effectiveness, and the behavior of social networks (*Sallach and Macal, 2001*; *Gilbert and Troitzsch, 2005*). In recent years, it has been introduced to the geosciences and other fields to provide novel ideas for the study of modern geography, including land use simulation and planning as well as residential choice and residential space differentiation (*Benenson et al., 2002*). The urban flood disaster system is a typical complex "natural and social" system. The introduction of ABM to simulate space-time distributions of populations is expected to quantify the dynamic exposure of populations to urban flood disasters. For example, *Dawson et al. (2011)* proposed a dynamic ABM for flood event management to evaluate population vulnerability under different storm surge conditions, dam break scenarios, flood warning times, and evacuation strategies.

3.3 Spatio-temporal simulation of population distribution

The individual travels were simulated using ABM by defining the activity patterns of different types of residents to subsequently obtain the distribution of the population at each moment. The ABM of residents' travels established in this study included two core elements of agents and activities, and two basic elements of blocks and networks. The travel survey data were used according to the demographic properties of the agent to generate synthetic daily routines.

Residents were independent individuals with subjectivity. This study abstracted them as agents. Only a limited number of agent classifications were used to reduce the number of agent types. The types of agents were classified according to the social characteristics of the residents. Age and gender characteristics mainly affect the ability of people to respond to disasters. The self-help abilities of the minors under 18 years of age and residents older than 60 years are generally poor. In the event of natural disasters, they are generally categorized as the objects of help. The middle-aged group (18–60 years old) generally has greater physical strength with better ability to cope with disasters. Unemployed people are more vulnerable to natural disasters. On the one hand, their living environments and resistance to disasters are poor; on the other hand, their economic conditions are limited, which impedes recovery after the disaster and seriously affects their daily life in the short term. Education level is related to the possibility of receiving early warning information by the individual. Individuals with higher education levels are more likely to respond to early warning information and are more aware of disasters than others (*Terti et al., 2015*; *Shabou et al., 2017*). Additionally, different travel modes have different effects on the activity patterns of people as well as on exposure levels when disasters occur. Therefore, the agent types were divided according to age, gender, employment status, education level, and travel mode.

Activities were classified as work, study, recreation, shopping, at-home, and travel.~~Activities were classified as work, learning, leisure, recreation, shopping, rest, and travel.~~ An activity pattern consisted of a series of activities to describe the spatio-temporal distribution of the agent. The location and scope of an agent were restricted to blocks and networks. Different types of agents indicated different activity patterns, and the same agent type could also indicate different activity patterns in different scenarios. To capture the variability in the travel survey and the uncertainties in behavior, synthetic daily routines were described in probabilistic terms. Figure 4 presents an example of the synthetic daily routine of an agent with the following demographic characteristics: ~~fe~~male agent, aged 18–60 years, and ~~un~~employed. In this example, the agent started the day at 8 am on a weekday. The agent then had a 0.8 probability of going straight to work~~traveled by a school to drop the children off~~, subsequently ~~had a 0.8 probability of shopping~~went home, and so on.

The study area was discretized into several blocks to improve the spatial resolution of the exposure results. The discretization procedure was conducted with geographic information system (GIS) tools (*Lü et al., 2018*), and several factors, including rivers, roads, land use, and buildings, were considered. Blocks were activity places for agents and represented the smallest unit of exposure. This study divided the block into five categories: residential area, school, company, recreational area, and others. Additionally, the residential areas were subdivided into I, II, III, and IV classes according to the type of building.

In this study, the network referred to roads and restricted the spatial travel scope of an intelligent agent. Rural roads, highways, and urban roads (including main roads, sub trunk roads, and its branches) were included in the network. The route selection criteria were defined once the different activities from each individual's schedule were located, and road section attributes were specified. Although various factors are involved in the route choice process, several studies have indicated that minimizing travel time is the principal criterion for selecting routes (*Papinski et al., 2009*;

Ramming, 2001; *Bekhor et al., 2006*). Therefore, the classical Dijkstra algorithm, a single-source shortest path algorithm that provides trees of minimal total length and time in a connected set of nodes, was selected in this study (*Dijkstra, 1959*). The activity pattern attributions concerned only the starting times and durations of the activity sequences, thus indicating that the travel duration for each individual was computed based on the distance between the different activity locations. Therefore, the implemented schedules may be distorted compared to the assigned schedules in terms of travel durations (*Terti et al., 2015*).

3.4 Impacts of disasters on anthropogenic activities

This study accounted for the adaptability or adjustment behavior of residents to disasters during the disaster event. The type of activity and its sensitivity to disaster affected the residents' disaster response behavior. Recreation and shopping activities were easier to cancel and postpone than work and learning (*Cools et al., 2010*). The sensitivities of residents to disasters depended on their socioeconomic characteristics and risk factors such as disaster- (flood-) related knowledge and experience. People with higher education levels are more knowledgeable about disasters and are more likely to receive early warning information and take effective measures (*Terti et al., 2015*). Additionally, it is easier for workers to ignore the risks of a disaster (*Ruin et al., 2007*; *Drobot et al., 2007*). Therefore, this study accounted for the impacts of education level on the response behavior of residents to disaster events.

The impacts of a disaster on population distribution were determined by defining different activity patterns and their changing probabilities. Figure 5 indicates activity patterns during different disaster scenarios for ~~un~~employed adult ~~wo~~men who had received higher education~~during different disaster scenarios~~. The "bad weather" scenario was similar to the "daily activity" pattern. For instance, the change in travel probability during “bad weather” due to a rainstorm reflected the adaptive behavior of residents. The “warning” scenario assumed that the government had issued early warning information at eight a.m., the schools had suspended classes during the weekday, and the resident responses were stronger than those to the “bad weather” scenario, thereby resulting in a greater difference in activity patterns.

3.5 Dynamic exposure assessment

The dynamic exposure was calculated based on the simulations of spatio-temporal distributions of the population and flooding. Therefore, the exposure at each moment was calculated according to the population distribution and flood data at that time. Based on the availability of data, this study focused only on three types of disaster-bearing bodies, i.e., population, roads, and buildings.

(i) Population

Population exposure generally refers to the population exposed to the impacts of disaster events and is characterized by regional population or population density. This study selected the exposed population and accounted for vulnerable groups and road users. Among these, age was the primary factor impacting the vulnerability. Specifically, the young (people under the age of 18 years) and the elderly (people over 60 years old) were the vulnerable groups.

(ii) Roads

As the basic skeleton of a city, roads are not only the media for daily travel of passengers and freight transportation but also disaster-bearing bodies (*Yin, et al., 2016a*), as they are vulnerable to flood disasters. This study selected the number and lengths of exposed roads to reflect road exposure.

(iii) Buildings

The aggravation of urban flooding has made building flooded more common in urban areas, thus resulting in loss of internal property and construction structure. Additionally, the dynamic state of building exposure is related to the safety of both the building as well as the nearby population. In this study, the area of the exposed building and the depth of accumulated water in the building were considered to be the building exposure.

3.6 Scenario design

The daily behaviors of people are characterized by certain patterns with regard to daily, weekly, monthly, and annual cycles. The rainstorm ("bad weather") and disaster response measures adopted by the organization ("warning") are likely to affect people's daily behaviors. Therefore, 12 scenarios, representing different flooding types and human activities, were designed in this study (Table 3). S1, S2, S7, and S8 were control groups that indicated human activity with no rain and no warning, while the rest of the scenarios were experimental groups.

4. Results

4.1 Model implementation and parameter setting

As an important spatial data management and analysis technology, GIS plays an important role in dynamic exposure analysis of urban floods. Because of the simplicity, readability and extensibility of the Python programming language, an increasing number of research institutes are adopting it for development. Therefore, the model was developed using the Visual Studio Code software (*Visual studio code, 2018*) and Python programming language (*Python, 2018*). The development of the graphical user interface (GUI), GIS module, and drawing module was realized by Qt (*Qt, 2018*), Geopandas (*Geopandas, 2018*), and Matplotlib (*Matplotlib, 2018*), respectively.

(i) Block generation

In this study, the study area was divided into 237 blocks based on the method introduced in Sect. 3.3. The block types and their spatial distributions are shown in Fig. 6 and Fig. 7, respectively. Most of the blocks in the study area were categorized as residential area, while blocks of recreational areas and others (which indicated rivers) were few and concentrated.

(ii) Parameter setting

Since the census did not identify individuals according to addresses, at the start of each simulation, an agent population with the same distributions of age, gender, employment, education level, and travel mode was randomly located within the residential area for the case study. The synthetic daily routines were described in probabilistic terms to capture the variability in the travel survey and uncertainties in behavior.

Additionally, to reduce the number of agent types, only a limited number of agent classifications were used. The distribution of population characteristics for Liandu District is shown in Table 4. The agents were divided into 18 types for daily (non-disaster) scenarios (S1, S2, S7, and S8) and 24 types for disaster scenarios (other scenarios except S1, S2, S7, and S8) based on the influence of education level on the individual disaster response behavior (Fig. 8).

(iii) Exposure threshold

Although flood fatalities can occur through a number of mechanisms, such as physical trauma, heart attack, or electrocution, drowning accounts for two-thirds of the fatalities (*Jonkman and*

Kelman, 2005). Previous research has established that the probability of death or serious injury as a result of exposure to flooding (*Abt et al., 1989*; *Karvonen et al., 2000*; *Lind et al., 2004*; *Jonkman and Penning‐Rowsell, 2008*) is dominated by (1) the depth of floodwater and (2) the velocity of floodwater. Additionally, the rate of water level rise can also play an important role in this regard. However, other factors, such as age, fitness level, height, and weight of the individual, are also important for determining their vulnerability to disasters. A comprehensive review of the flood-related casualty data and methods to assess the risk of death or serious harm to people caused by flooding is provided by the *Department for Environment Food and Rural Affairs and Environment Agency (2003)* and *Jonkman and Penning‐Rowsell (2008)*. In this study, rather than predicting mortality (which is subject to random factors as well as those mentioned previously), exposure to floodwater depths of 25 cm or greater under relatively fast flowing (2.5 m/s or greater) conditions was established as the threshold for most vulnerable people (*DEFRA and Environment Agency, 2003*). This provided a conservative estimate of individuals vulnerable to floodwater rather than an estimate of mortality (*Dawson et al., 2011*).

Since building steps (thresholds) exert a blocking effect on shallow flooding, they are likely to reduce the degree of flooding by restricting the flood water to the outside of the building, thereby reducing the exposure of the building. Therefore, this study assigned building step heights to corresponding block types according to the architectural design standards of China and the actual conditions of the study area (Table 5). It should be noted that the block type “Other” constituted rivers and did not contain buildings. Therefore, the exposure of the building was determined according to the depth of the flood and the height of the building steps. The depth of the water entering the building was the difference between the depth of the flood and the height of the step.

4.2 Flood simulation

Figure 9 indicates the accumulated water depths and velocities of pluvial and fluvial floods in the study area. As is evident, the pluvial and fluvial floods exerted significant impacts, and the urban area near the Oujiang River was the most severely flooded area. Additionally, water is also accumulated in the inner areas of the city, mainly on roads, in case of pluvial flood disasters. The variations in water depths and velocities for eight severely flooded areas (including blocks and roads) are presented in Fig. 10. As indicated, evident spatio-temporal variations in flooding were observed. Figures 9 and 10 indicate that water depth was the main factor causing life and property losses, whereas water velocity had little or no effect.

The flooded urban roads and locations in Lishui during the 50-year flood in 2014 were as follows: the city had 10 flooded roads and 18 water accumulation points. The actual hydrological points were selected and combined with the urban flooding results simulated by the prototype system. The water accumulation distribution is indicated in Fig. 1~~6~~1.

To avoid overlapping with the simulated water accumulation results for roads, the actual flooding points in the figure only included road junctions and the entirety of Gucheng road (the Lutang Street to Dayou Street section), and Liyang Street (which connected the senior middle school to the Sanyan temple section) was represented by corresponding intersection points. Figure 1~~6~~ 1 indicates that both the simulation results and the actual water accumulation points were mainly distributed along the river. The simulated water accumulation area (Fig. ~~16~~11(a)) included roads in the center of the city and was larger than the actual flooding area. This difference could be attributed to different definitions of "water accumulation". The simulation results presented in Figure 1~~6~~1 included all areas where the accumulated water depth during the flooding period was greater than 15 cm. The actual water accumulation point was defined as one experiencing rainfall greater than 50 mm over a 24 hour period. Additionally, it was characterized by the water accumulation depth of the road reaching 15 cm (the meteorological department issued the blue rainstorm warning at this level), the water withdrawal time reaching one hour, and the water accumulation scope value being greater than 50 m^2. Certain gaps existed between the observational data and the actual flow since the observation station was far from the study area. Hence, the results indicated that the simulated water accumulation area during the fluvial flood (Fig. 1~~6~~1 (b)) was smaller than that of the actual situation.

4.3 Simulation of the spatio-temporal distribution of population

The population spatio-temporal distribution was simulated based on six scenarios: (1) daily, weekday (S1, S7); (2) daily, weekend (S2, S8); (3) bad weather, weekday (S3, S9); (4) bad weather, weekend (S4, S10); (5) warning, weekday (S5, S11); (6) warning, weekend (S6, S12). Figure 1~~0~~2 indicates the population variation for blocks and roads for the six scenarios. Figure ~~11~~12(a) indicates that, among the three weekend scenarios, the population in the playground (Block 77) changed more than the population in the company (Block 113). Figure ~~11~~12(b) indicates that the population on the roads was volatile, and the morning peak hour during the weekend was delayed by an hour in comparison to that during the weekdays. The population distribution in the study area is shown in Fig. ~~12~~13. The population was unevenly distributed and concentrated in recreational and residential areas over the weekend. However, the population distribution on weekdays was relatively uniform. The concurrent population distribution for the six scenarios changed significantly during the weekend, while the distribution for weekdays changed little.

Figures ~~11~~ 12 and ~~12~~ 13 indicate that the population change patterns were different for different blocks types. The daily routines of several people started from the residential area (home) in the morning, followed by school or company blocks during weekdays and recreational areas during weekends, and, finally, concluded with a return to the residential area at night. During the occurrence of rainstorms or the reception of warning messages, different types of people reacted differently (continuing, postponing, or cancelling the originally planned activities). Vulnerable people, like the elderly and children, and sensitive people (such as the homeless) were more likely to cancel travel plans. Additionally, recreational activities were more likely to be cancelled than were learning and work activities.

The reliability of the simulation of the spatio-temporal population distribution was indirectly verified by utilizing the traffic flow data from June 24 to July 7, 2017. The morning and evening peak hours on weekdays and weekends, the simulated total number of residents passing the four intersections (such as the junction of the Liqing and Huayuan roads) during peak hours, and the actual measured traffic flow at the intersections are shown in Fig. 1~~7~~4. The traffic flow data in Fig. 1~~7~~4 are multi-day average results.

In theory, the simulated value should be much larger than the measured value since the former indicates the number of people while the latter represents the number of cars and buses. However, as indicated in Fig. 1~~7~~4, the simulated value was close to the measured value. This could be attributed to the assumption that the study area was closed and the simulated population was the number of permanent residents, excluding the migrant population. In reality, the number of migrants in the urban area during daytime is large owing to its geographical location. Moreover, this study simplified human activities when simulating the spatio-temporal distribution of the population. Therefore, the number of pedestrians on the road was small. However, both the simulated and measured values were essentially similar with regard to changes in their trends. Therefore, the simulation method for the spatio-temporal distribution of population is feasible, and the results are reliable.

4.4 Exposure assessment

Figure ~~13~~ 15 presents the population exposure variation for two selected areas. The difference between pluvial and fluvial flood scenarios could be attributed to differences in the changes and degrees of water accumulation. Figure ~~13~~15(a) indicates that population exposure was the highest for the daily scenario, followed by the bad weather scenario and minimum warning scenario. However, as indicated in Fig. ~~13~~15(b), the population was most exposed to both weekend and weekday warning scenarios. This is attributed to the assumption that the disaster response behavior adopted by residents was to reduce travel, i.e., the refuge of residents was the residential area. Additionally, the response was not based on the exposure of the residential area. Therefore, when residential areas, such as Block 6, were exposed to floods, the residents chose to reduce travel, thus resulting in an increase in the population of residential areas and consequently increasing the population exposure. According to the analysis of the 12 scenarios, the government departments can carry out disaster prevention and mitigation measures for areas with large amounts of population exposure, such as evacuation prior to the disaster, and initiate key rescue operations during the disaster. The method proposed in this study can also help determine vulnerable populations and road users in the exposed blocks. Because we had considered vulnerable people and road users when we constructed the population groups (agents), we can get similar information from the results of vulnerable populations and road users in the exposed blocks, like the exposed population. Such information is of great practical significance.

Figure ~~14~~ 16 presents variations in the road and building exposures of two selected areas with serious flooding. The road and building exposures for the study area are presented in Fig. ~~15~~17. It can be concluded that road and building exposures during pluvial and fluvial floods also varied with the flood depth. Additionally, the exposed road length of the block was fluctuant, while the building was either entirely exposed or not exposed. Furthermore, the area of the road affected by pluvial and fluvial floods was greater than that of the buildings. As indicated in Fig. ~~15~~17, exposed buildings were present only in a few areas (blocks), while roads were affected in several areas. Additionally, buildings were least exposed due to high thresholds or the number of building steps designed and built in recent years, while roads and population were severely affected by floods.

~~4.5 Validation~~

~~The flooded urban roads and locations in Lishui during the 50-year flood in 2014 were as follows: the city had 10 flooded roads and 18 water accumulation points. The actual hydrological points were selected and combined with the urban flooding results simulated by the prototype system. The water accumulation distribution is indicated in Fig. 16.~~

~~To avoid overlapping with the simulated water accumulation results for roads, the actual flooding points in the figure only included road junctions and the entirety of Gucheng road (the Lutang Street to Dayou Street section), and Liyang Street (which connected the senior middle school to the Sanyan temple section) was represented by corresponding intersection points. Figure 16 indicates that both the simulation results and the actual water accumulation points were mainly distributed along the river. The simulated water accumulation area (Fig. 16(a)) included roads in the center of the city and was larger than the actual flooding area. This difference could be attributed to different definitions of "water accumulation". The simulation results presented in~~

~~Figure 16 included all areas where the accumulated water depth during the flooding period was greater than 15 cm. The actual water accumulation point was defined as one experiencing rainfall greater than 50 mm over a 24-hour period. Additionally, it was characterized by the water accumulation depth of the road reaching 15 cm (the meteorological department issued the blue rainstorm warning at this level), the water withdrawal time reaching one hour, and the water accumulation scope value being greater than 50 m^2. Certain gaps existed between the observational data and the actual flow since the observation station was far from the study area. Hence, the results indicated that the simulated water accumulation area during the fluvial flood (Fig. 16 (b)) was smaller than that of the actual situation.~~

~~The reliability of the simulation of the spatio-temporal population distribution was indirectly verified by utilizing the traffic flow data from June 24 to July 7, 2017. The morning and evening peak hours on weekdays and weekends, the simulated total number of residents passing the four intersections (such as the junction of the Liqing and Huayuan roads) during peak hours, and the actual measured traffic flow at the intersections are shown in Fig. 17. The traffic flow data in Fig. 17 are multi-day average results.~~

~~In theory, the simulated value should be much larger than the measured value since the former indicates the number of people while the latter represents the number of cars and buses. However, as indicated in Fig. 17, the simulated value was close to the measured value. This could be attributed to the assumption that the study area was closed and the simulated population was the number of permanent residents, excluding the migrant population. In reality, the number of migrants in the urban area during daytime is large owing to its geographical location. Moreover, this study simplified human activities when simulating the spatio-temporal distribution of the population. Therefore, the number of pedestrians on the road was small. However, both the~~

~~simulated and measured values were essentially similar with regard to changes in their trends. Therefore, the simulation method for the spatio-temporal distribution of population is feasible, and the results are reliable.~~

5. Conclusions

Urban flooding considerably impacts the daily lives of residents and not only affects commuting but also causes casualties and traffic congestion. This study proposed a method for obtaining high-resolution dynamic exposure to urban flooding. First, the spatio-temporal distributions of pluvial and fluvial floods were simulated by the LISFLOOD-FP model. Second, the responses of residents to bad weather and government measures (warnings) were incorporated to develop an ABM to simulate residents' activities during flooding. Finally, urban exposure during different flood scenarios was comprehensively simulated and was based on the population and hydrological simulation results, road and building data, and the case study of the Lishui urban district.

The method developed could predict floods as well as the exposure of buildings, roads, and the population at different times and locations. Additionally, it could provide effective reference information for residents' travels and urban disaster management. In summary, this study had four main elements. First, different spatio-temporal distributions of water depth and velocity predictions were obtained using the LISFLOOD-FP model. Second, an ABM was utilized to simulate the spatio-temporal distributions of the population. Third, the impacts of pluvial and fluvial floods on buildings were found to be small, while that on roads and the population was evident. Finally, if residents simply reduced their travels (stayed at home), the exposure of the population in the exposed residential areas increased.

It should be noted that there is no comprehensive way to verify the proposed method. This is because parameters of human behavior and psychological processes are difficult (or, to some extent, impossible) to obtain. In this study, the proposed method was verified indirectly. The actual traffic information for each road intersection was collected and compared with the simulated population results. Additionally, the information for actual water accumulation points was compared with the simulated water accumulation results. However, a few limitations persist. For instance, considerable uncertainties regarding the use and design of the ABM exist. These include differences in the responses of residents of the same type to disasters in the same scenario. Therefore, this study simply attempted to reflect reality. Moreover, simplification of the behavior patterns and disaster responses of residents is inevitable, thus resulting in differences between the simulation results and reality. In addition, the investigation of different durations and intensities of the rainstorm is also relevant. However, the inclusion of other factors was beyond the scope of this research. Therefore, future studies should focus on optimizing the proposed method and incorporating the effects of different durations and intensities of rainstorms.

Acknowledgements

This study is supported by the National Natural Science Foundation of China (Nos：41771424, 41871299) and National Key R & D Program of China (Nos: 2018YFB0505500, 2018YFB0505502). Dawei Han and Lu Zhuo are supported by Newton Fund via Natural Environment Research Council (NERC) and Economic and Social Research Council (ESRC) (NE/N012143/1).

References

Abt, S. , Wittier, R. , Taylor, A. and Love, D.: HUMAN STABILITY IN A HIGH FLOOD HAZARD ZONE1. JAWRA Journal of the American Water Resources Association, 25: 881-890, https://doi.org/10.1111/j.1752-1688.1989.tb05404.x, 1989.

Atta-Ur-Rahman, D.: Disaster risk management, 2014.

Axelrod, R.: The complexity of cooperation: Agent-based models of competition and collaboration (Vol. 3). Princeton University Press, 1997.

Bates, P. D., and De Roo, A. P. J.: A simple raster-based model for flood inundation simulation. Journal of hydrology, 236(1-2), 54-77, https://doi.org/10.1016/S0022-1694(00)00278-X, 2000.

Bates, P., Trigg, M., Neal, J., Dabrowa ,A.: LISFLOOD-FP User manual, Code release 5.9.6, School of Geographical Sciences, University of Bristol, University Road, Bristol, BS8 1SS, UK, 2013. Available online at University of https://www.bristol.ac.uk/media-library/sites/geography/migrated/documents/lisflood-manual-v5.9.6.pdf.

Bekhor, S., Ben-Akiva, M. E., and Ramming, M. S.: Evaluation of choice set generation algorithms for route choice models. Annals of Operations Research, 144(1), 235-247, https://doi.org/10.1007/s10479-006-0009-8, 2006.

Benenson, I., Omer, I., and Hatna, E.: Entity-based modeling of urban residential dynamics: the case of Yaffo, Tel Aviv. Environment and Planning B: Planning and Design, 29(4), 491-512, https://doi.org/10.1068/b1287, 2002.

Brunner, G. W.: HEC-RAS River Analysis System User's Manual Version 4.0. US Army Corps of Engineers, Hydrologic Engineering Center. Report CPD-68, 2008.

Cen, G., Shen, J., and Fan, R.: Research on rainfall pattern of urban design storm. Advances in Water Science, 9(1), 41-46, https://doi.org/10.14042/j.cnki.32.1309.1998.01.007, 1998.

Charley, W., Pabst, A., Peters, J.: The Hydrologic Modeling System (HEC-HMS): Design and Development Issues. Hydrological Engineering Center, US Army Corps of Engineers, Technical Paper No. 149, 1995.

Chen, Y., Zhou, H., Zhang, H., Du, G., and Zhou, J.: Urban flood risk warning under rapid urbanization. Environmental research, 139, 3-10, https://doi.org/10.1016/j.envres.2015.02.028, 2015.

Cools, M., Moons, E., Creemers, L., and Wets, G.: Changes in travel behavior in response to weather conditions: do type of weather and trip purpose matter?. Transportation Research Record: Journal of the Transportation Research Board, (2157), 22-28, https://doi.org/10.3141/2157-03, 2010.

Danish Hydraulic Institute (DHI).: MIKE SHE Water movement user manual. DHI Water & Environment, 2000.

Dankers, R., and Feyen, L.: Climate change impact on flood hazard in Europe: An assessment based on high‐resolution climate simulations. Journal of Geophysical Research: Atmospheres, 113(D19), https://doi.org/10.1029/2007JD009719, 2008.

Dawson, R. J., Peppe, R., and Wang, M.: An agent-based model for risk-based flood incident management. Natural hazards, 59(1), 167-189, https://doi.org/10.1007/s11069-011-9745-4, 2011.

DEFRA and Environment Agency.: Flood risks to people phase 1: R&D Technical Report FD2317. DEFRA, London, 2003.

Dijkstra, E. W.: A note on two problems in connexion with graphs. Numerische mathematik, 1(1), 269-271, 1959.

Drobot, S. D., Benight, C., and Gruntfest, E. C.: Risk factors for driving into flooded roads. Environmental Hazards, 7(3), 227-234, https://doi.org/10.1016/j.envhaz.2007.07.003, 2007.

Gain, A. K., Mojtahed, V., Biscaro, C., Balbi, S., and Giupponi, C.: An integrated approach of flood risk assessment in the eastern part of Dhaka City. Natural Hazards, 79(3), 1499-1530, https://doi.org/10.1007/s11069-015-1911-7, 2015.

Geopandas: http://geopandas.org/, 2018.

Gilbert, N., and Troitzsch, K.: Simulation for the social scientist. McGraw-Hill Education (UK), 2005.

Guo, E., Zhang, J., Ren, X., Zhang, Q., and Sun, Z.: Integrated risk assessment of flood disaster based on improved set pair analysis and the variable fuzzy set theory in central Liaoning Province, China. Natural hazards, 74(2), 947-965, https://doi.org/10.1007/s11069-014-1238-9, 2014.

Hammond, M. J., Chen, A. S., Djordjević, S., Butler, D., and Mark, O.: Urban flood impact assessment: A state-of-the-art review. Urban Water Journal, 12(1), 14-29, https://doi.org/10.1080/1573062X.2013.857421, 2015.

Havnø, K., Madsen, M. N., and Dørge, J.: MIKE 11–a generalized river modelling package. Computer models of watershed hydrology, 733-782, 1995.

Horritt, M. S., and Bates, P. D.: Evaluation of 1D and 2D numerical models for predicting river flood inundation. Journal of hydrology, 268(1-4), 87-99, https://doi.org/10.1016/S0022-1694(02)00121-X, 2002.

Huang, H., Fan, Y., Yang, S., Li, W., Guo, X., Lai W., and Wang H.: A multi-agent based theoretical model for dynamic flood disaster risk assessment. Geographical Research, 34(10):1875-1886, https://doi.org/10, 1875-1886, 10.11821/dlyj20151006, 2015.

IPCC.: Summary for Policymakers. In: Managing the Risks of Extreme Events and Disasters to Advance Climate Change Adaptation. A Special Report of Working Groups I and II of the Intergovernmental Panel on Climate Change. Cambridge University Press, Cambridge, UK, and New York, NY, USA, pp. 3-21, 2012.

Johnstone, M. A.: Life safety modelling framework and performance measures to assess community protection systems: application to tsunami emergency preparedness and dam safety management, Ph.D. thesis, University of British Columbia, 2012.

Jonkman, S. N., and Kelman, I.: An analysis of the causes and circumstances of flood disaster deaths. Disasters, 29(1), 75-97, https://doi.org/10.1111/j.0361-3666.2005.00275.x, 2005.

Jonkman, S. N., and Penning‐Rowsell, E.: Human Instability in Flood Flows 1. JAWRA Journal of the American Water Resources Association, 44(5), 1208-1218, https://doi.org/10.1111/j.1752-1688.2008.00217.x, 2008.

Kang, T., Zhang, X., Zhao, Y.,Wang, Y., and Zhang, W.: Agent-based Urban Population Distribution Model. Scientia Geographica Sinica, 32(7): 90-797, https://doi.org/10.13249/j.cnki.sgs.2012.07.003, 2012.

Karvonen, R. A., Hepojoki, A., Huhta, H. K., and Louhio, A.: The use of physical models in dam-break analysis. RESCDAM Final Report. Helsinki University of Technology, Helsinki, Finland, 2000.

Liang, Y., Wen, J., Du, S., Xu, H., and Yan J.: Spatial-temporal Distribution Modeling of Population and its Applications in Disaster and Risk Management. Journal of Catastrophology, 30(04):220-228, https://doi.org/ 10.3969/j.issn.1000-811X.2015.04.038, 2015.

Lind, N., Hartford, D., and Assaf, H.: Hydrodynamic models of human stability in a flood 1. JAWRA Journal of the American Water Resources Association, 40(1), 89-96, https://doi.org/10.1111/j.1752-1688.2004.tb01012.x, 2004.

Lindberg, S., Nielsen, J. B., and Carr, R.: An integrated PC-modelling system for hydraulic analysis of drainage systems. In Watercomp'89: The First Australasian Conference on Technical Computing in the Water Industry; Preprints of Papers (p. 127). Institution of Engineers, Australia, 1989.

Lü, G., Batty, M., Strobl, J., Lin, H., Zhu, A. X., and Chen, M.: Reflections and speculations on the progress in Geographic Information Systems (GIS): a geographic perspective. International Journal of Geographical Information Science, 1-22, https://doi.org/10.1080/13658816.2018.1533136, 2018.

Mahe, G., Paturel, J. E., Servat, E., Conway, D., and Dezetter, A.: The impact of land use change on soil water holding capacity and river flow modelling in the Nakambe River, Burkina-Faso. Journal of Hydrology, 300(1-4), 33-43, https://doi.org/10.1016/j.jhydrol.2004.04.028, 2005.

Mansur, A. V., Brondízio, E. S., Roy, S., Hetrick, S., Vogt, N. D., and Newton, A.: An assessment of urban vulnerability in the Amazon Delta and Estuary: a multi-criterion index of flood exposure, socio-economic conditions and infrastructure. Sustainability Science, 11(4), 625-643, https://doi.org/10.1007/s11625-016-0355-7, 2016.

Matplotlib: https://matplotlib.org/, 2018.

Moel, H. D., Aerts, J. C., and Koomen, E.: Development of flood exposure in the Netherlands during the 20th and 21st century. Global Environmental Change, 21(2), 620-627, https://doi.org/10.1016/j.gloenvcha.2010.12.005, 2011.

Nasiri, H., Mohd Yusof, M.J., and Mohammad Ali, T.A.: An overview to flood vulnerability assessment methods. Sustain. Water Resour. Manag., 2: 331, https://doi.org/10.1007/s40899-016-0051-x, 2016.

Papinski, D., Scott, D. M., and Doherty, S. T.: Exploring the route choice decision-making process: A comparison of planned and observed routes obtained using person-based GPS.

Transportation research part F: traffic psychology and behaviour, 12(4), 347-358, https://doi.org/10.1016/j.trf.2009.04.001, 2009.

Parker, D., Fordham, M., Tunstall, S., and Ketteridge, A. M.: Flood warning systems under stress in the United Kingdom. Disaster Prevention and Management: An International Journal, 4(3), 32-42, https://doi.org/10.1108/09653569510088050, 1995.

Python: https://www.python.org/, 2018.

Qt: https://www.qt.io/, 2018.

Ramming, M. S.: Network knowledge and route choice, Unpublished Ph. D. Thesis, Massachusetts Institute of Technology, 2001.

Rossman, L. A.: Storm water management model user's manual Version 5.1 EPA-600/R-14/413b[z]. National Risk Management Laboratory Laboratory Office of Research and Development U. S. Environmental Protection Agency, 2015. Available online at https://nepis.epa.gov/Exe/ZyPDF.cgi/P100N3J6.PDF?Dockey=P100N3J6.PDF

Röthlisberger, V., Zischg, A. P., and Keiler, M.: Identifying spatial clusters of flood exposure to support decision making in risk management. Science of the total environment, 598, 593-603, https://doi.org/10.1016/j.scitotenv.2017.03.216, 2017.

Ruin, I., Gaillard, J. C., and Lutoff, C.: How to get there? Assessing motorists' flash flood risk perception on daily itineraries. Environmental hazards, 7(3), 235-244, https://doi.org/10.1016/j.envhaz.2007.07.005, 2007.

Sallach, D. L., and Macal, C. M.: Introduction: The simulation of social agents. Social Science Computer Review, 19(3), 245-248, https://doi.org/10.1177/089443930101900301, 2001.

Shabou, S., Ruin, I., Lutoff, C., Debionne, S., Anquetin, S., Creutin, J. D., and Beaufils, X.: MobRISK: a model for assessing the exposure of road users to flash flood events. Natural Hazards and Earth System Sciences, 17(9), 1631, https://doi.org/10.5194/nhess-17-1631-2017, 2017.

Shi, P.: Theory and practice of disaster study. Journal of Natural Disasters, 4, 8-19, 1996.

Terti, G., Ruin, I., Anquetin, S., and Gourley, J. J.: Dynamic vulnerability factors for impact-based flash flood prediction. Natural Hazards, 79(3), 1481-1497. https://doi.org/10.1007/s11069-015-1910-8, 2015.

Visual studio code: https://code.visualstudio.com/, 2018.

Wan, H., Wang, J.: Analysis of Public Adaptive Behaviors to Drought and Flood Disasters in Middle Reaches of Weihe River:A Case Study on Qishan County of Shaanxi Province. Acta Agriculturae Jiangxi, https://doi.org/10.19386/j.cnki.jxnyxb.2017.05.21, 2017.

Weis, S. W. M., Agostini, V. N., Roth, L. M., Gilmer, B., Schill, S. R., Knowles, J. E., and Blyther, R.: Assessing vulnerability: an integrated approach for mapping adaptive capacity, sensitivity, and exposure. Climatic Change, 136(3-4), 615-629, https://doi.org/10.1007/s10584-016-1642-0, 2016.

Werren, G., Reynard, E., Lane, S. N., and Balin, D.: Flood hazard assessment and mapping in semi-arid piedmont areas: a case study in Beni Mellal, Morocco. Natural Hazards, 81(1), 481-511, https://doi.org/10.1007/s11069-015-2092-0, 2016.

Yang, X., Yue, W., and Gao, D.: Spatial improvement of human population distribution based on multi-sensor remote-sensing data: an input for exposure assessment. International journal of remote sensing, 34(15), 5569-5583, https://doi.org/10.1080/01431161.2013.792970, 2013.

Yin, Z.: Research of urban natural disaster risk assessment and case study, Ph.D. thesis, East china normal university, Shanghai, China, 2009.

Yin, J., Yu, D., and Wilby, R.: Modelling the impact of land subsidence on urban pluvial flooding: A case study of downtown Shanghai, China. Science of the Total Environment, 544, 744-753, https://doi.org/10.1016/j.scitotenv.2015.11.159, 2016a.

Yin, W., Yu, H., Cui, S., and Wang, J.: Review on methods for estimating the loss of life induced by heavy rain and floods. Progress in Geography, 35(2), 148-158, https://doi.org/10.18306/dlkxjz.2016.02.002, 2016b.

Figure 1. Location of the study area (left) and a digital elevation model indicating the specific details of the study area (right).

Figure 2. Overview of the dynamic exposure simulation to urban flooding.

Figure 3. Rainfall simulation results based on the CHM method, and observational data used for fluvial flood simulation.

Figure 4. A synthetic daily routine generated from the travel survey and census data for an ~~un~~employed ~~fe~~male agent aged 18–60 years.

Figure 5. Activity patterns for an ~~un~~employed ~~fe~~male agent aged 18–60 years and highly educated during disaster scenarios. (a) Bad weather (weekday) (b) Warning (weekday) (c) Bad weather (weekend) (d) Warning (weekend).

Figure 6. Number of different block types.

Figure 7. Spatial distribution of blocks.

Figure 8. Agent types for daily and disaster scenarios. Daily scenarios refers to S1, S2, S7, and S8. Others are disaster scenarios.

Figure 9. Accumulated water depths and velocities. T means time here.

Figure 10. Changes in the surface water depths and velocities for eight severely flooded areas. The “dep” indicates water depth, and “vel” indicates water velocity.

Figure 1~~6~~1. Map of the flooded area indicating the flooding simulation and the real flood in 2014. The information for the flooded area was provided by Lishui City Housing and Urban-Rural Construction Bureau.

Figure ~~11~~12. Population changes in blocks and roads for the six scenarios.

Figure ~~12~~13. Population distribution for the six scenarios. T means time here.

Figure 1~~7~~4. Traffic flow and population simulation results during peak hours on weekdays and weekends. The traffic flow data were provided by the Lishui City Traffic Bureau. Real means measured value here. LQ is Liqing Road, KF is Kaifa Road, HY is Huayuan Road, ZJ is Zijin Road, and LT is Lutang Street.

Figure ~~13~~15. Changes in the population exposure of two blocks for the 12 scenarios. Block 168 was a recreational area, and Block 6 was a residential area.

Figure ~~14~~16. Changes in road and building exposures in severely flooded blocks. The exposed road length and building area represent road and building exposures, respectively.

Figure ~~15~~17. Map of road and building exposures. T means time here.

~~**Figure 16.** Map of the flooded area indicating the flooding simulation and the real flood in 2014. The information for the flooded area was provided by Lishui City Housing and Urban-Rural Construction Bureau.~~

~~**Figure 17.** Traffic flow and population simulation results during peak hours on weekdays and weekends. The traffic flow data were provided by the Lishui City Traffic Bureau. Real means measured value here. LQ is Liqing Road, KF is Kaifa Road, HY is Huayuan Road, ZJ is Zijin Road, and LT is Lutang Street.~~

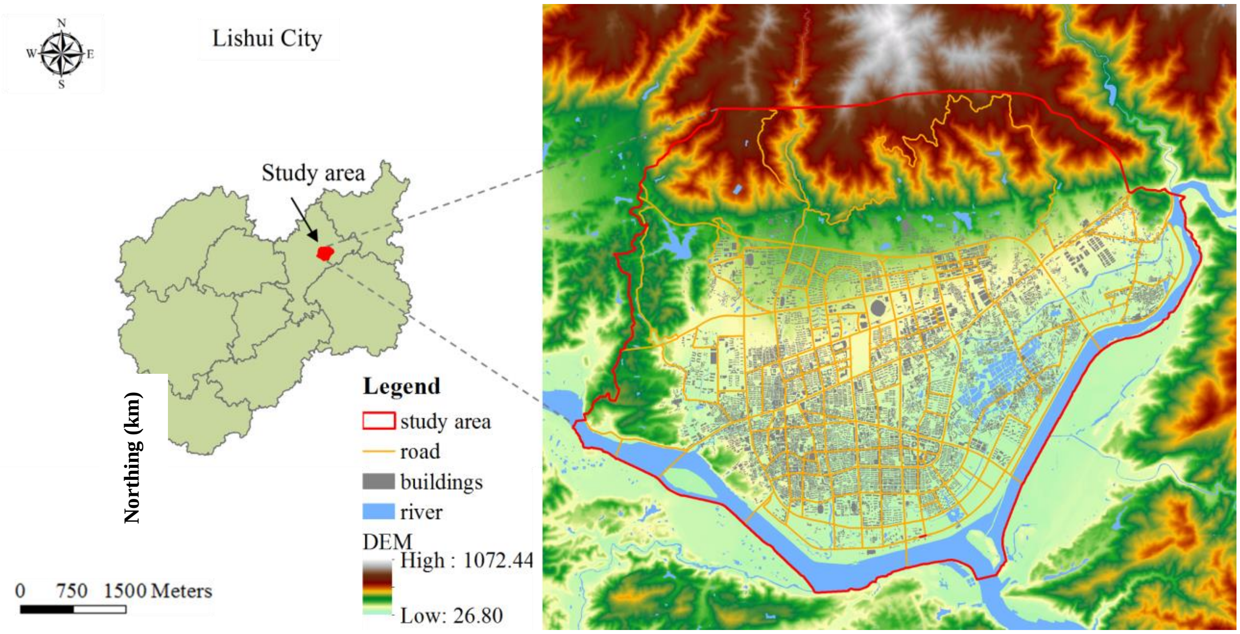

Figure 1. Location of the study area (left) and a digital elevation model indicating the specific details of the study area (right).

739

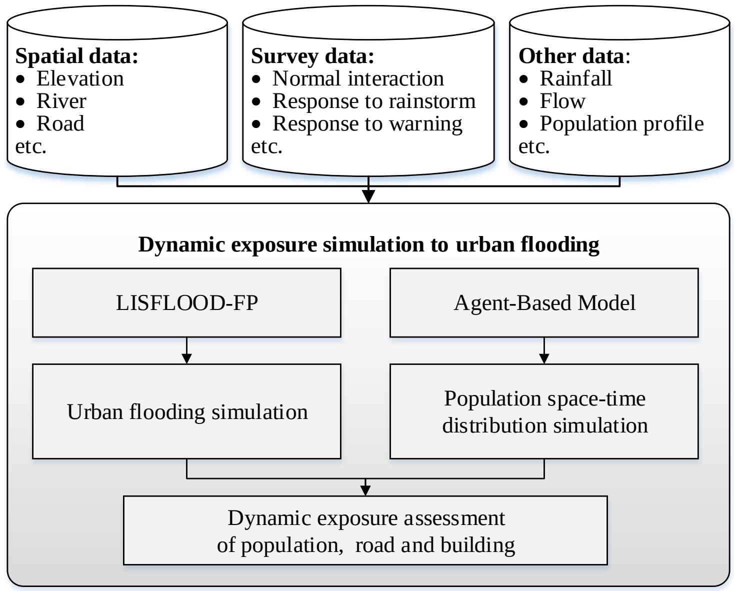

740 **Figure 2.** Overview of the dynamic exposure simulation to urban flooding.

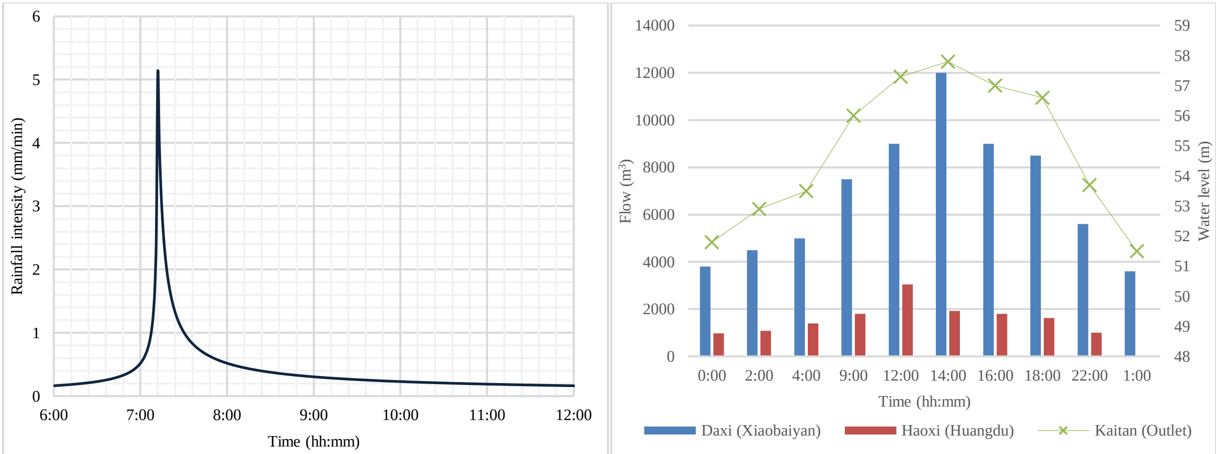

(a) Rainfall simulation data (b) Observational data

Figure 3. Rainfall simulation results based on the CHM method, and observational data used for fluvial flood simulation.

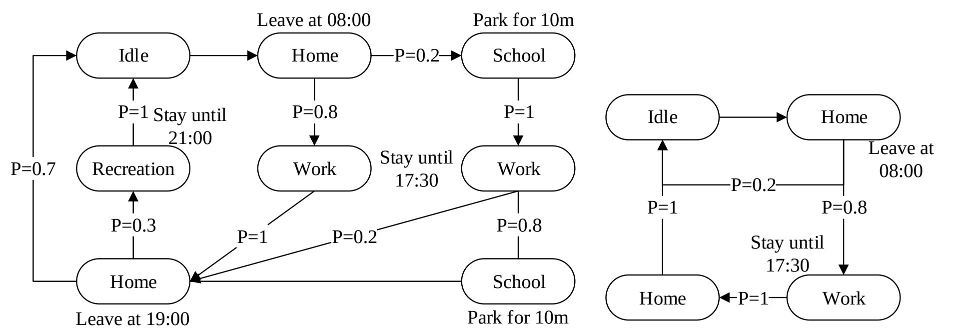

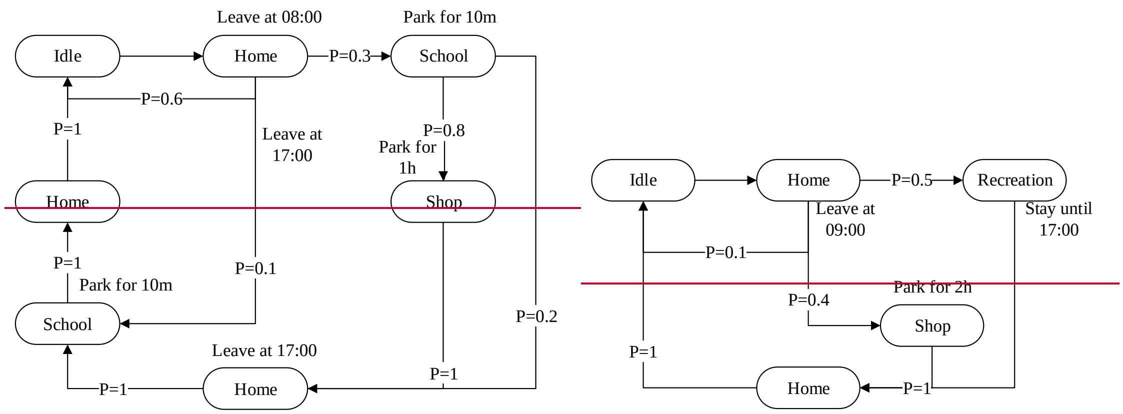

(a) Activity on weekdays (b) Activity on weekends

Figure 4. A synthetic daily routine generated from the travel survey and census data for an ~~un~~employed ~~fe~~male agent aged 18–60 years.

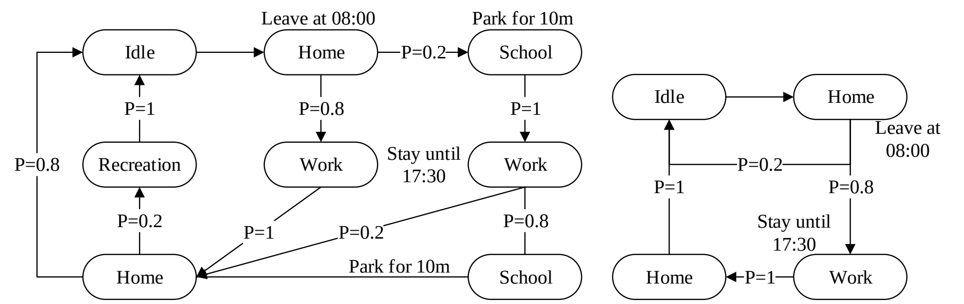

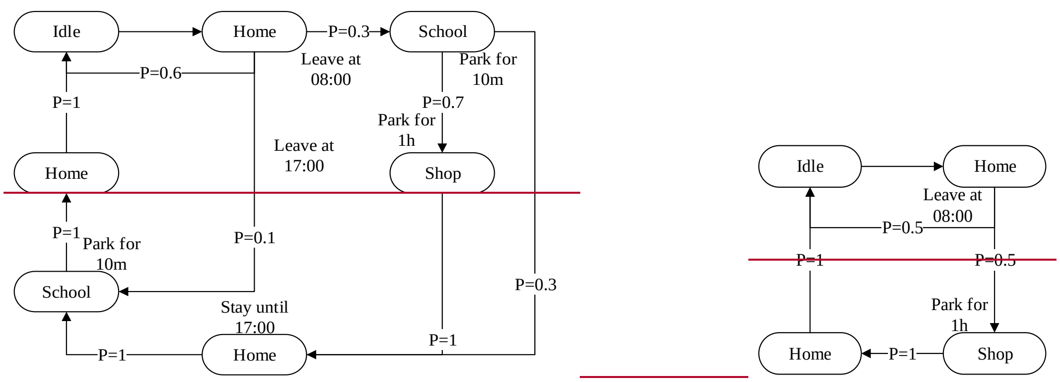

(a) Bad weather (weekday) (b) Warning (weekday)

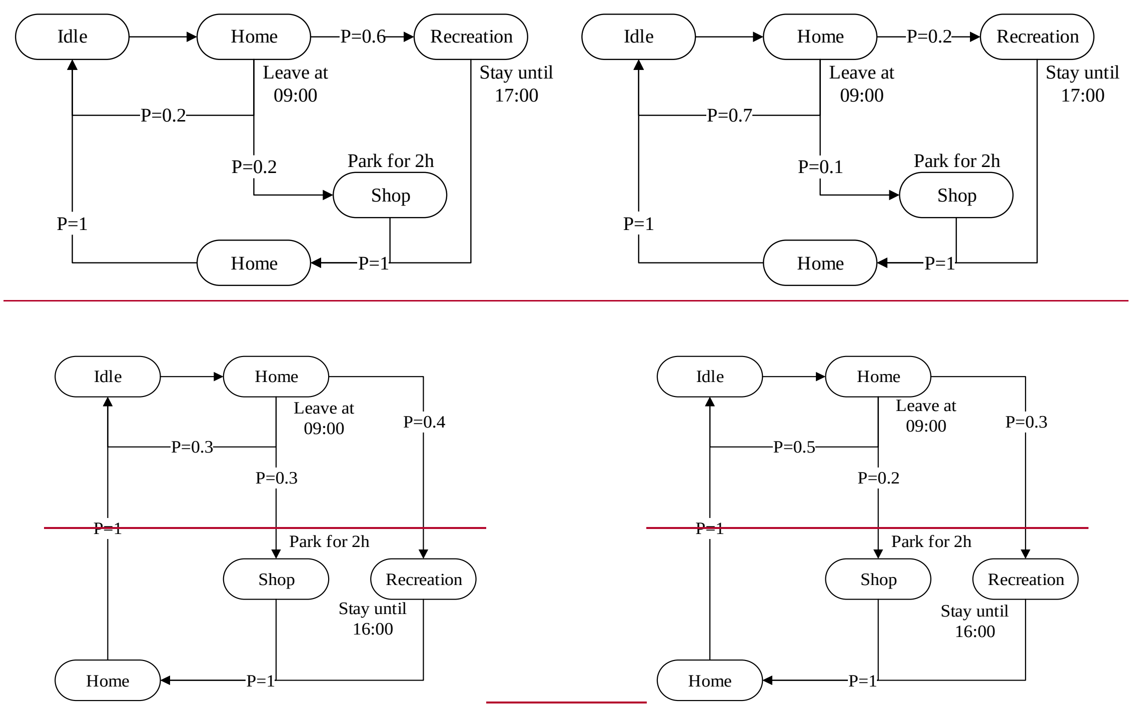

(c) Bad weather (weekend) (d) Warning (weekend)

Figure 5. Activity patterns for an ~~un~~employed ~~fe~~male agent aged 18–60 years <u>and highly educated</u> during disaster scenarios. (a) Bad weather (weekday) (b) Warning (weekday) (c) Bad weather (weekend) (d) Warning (weekend).

760

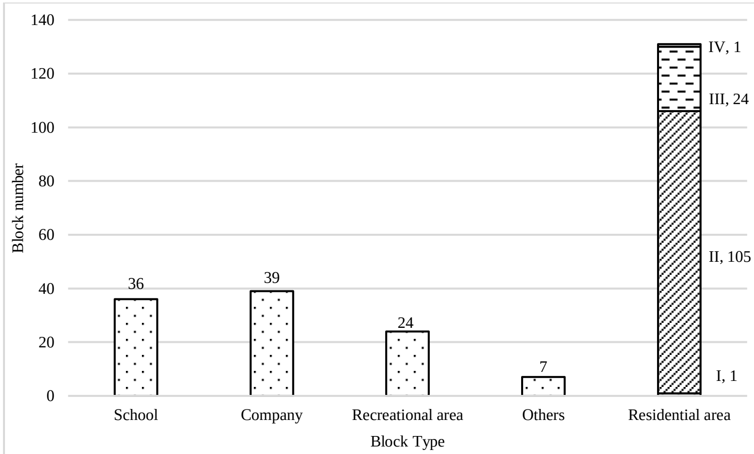

761 **Figure 6.** Number of different block types.

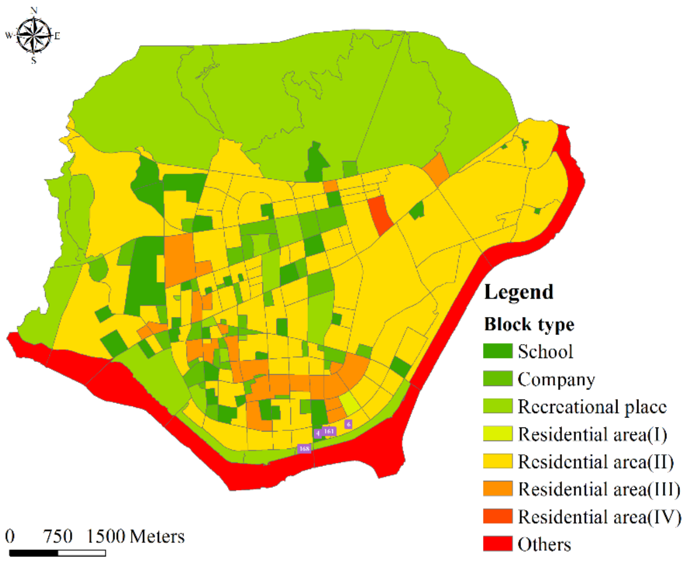

Figure 7. Spatial distribution of blocks.

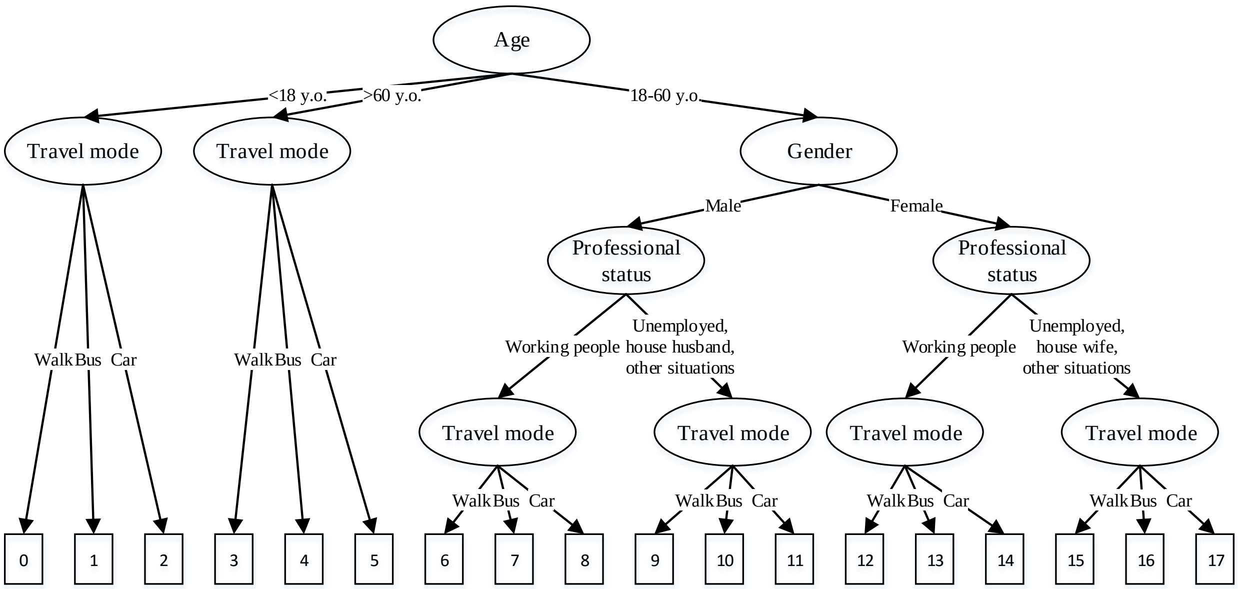

(a) Agent types for daily scenarios

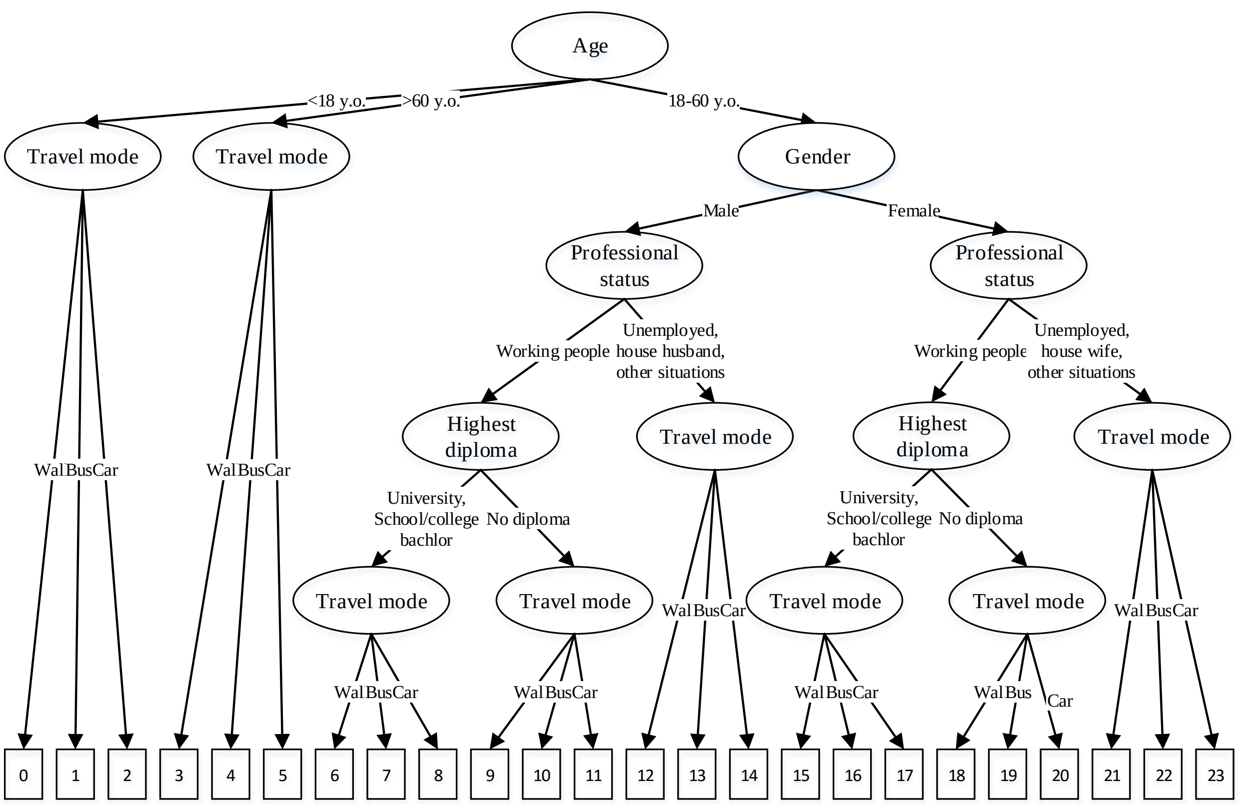

(b) Agent types for disaster scenarios

Figure 8. Agent types for daily and disaster scenarios. Daily scenarios refers to S1, S2, S7, and S8. Others are disaster scenarios.

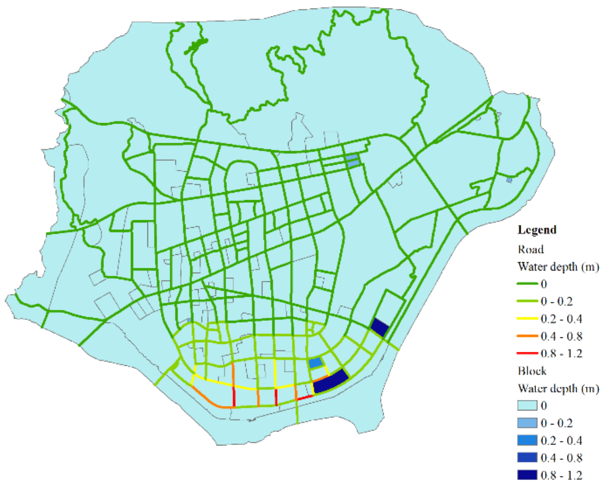

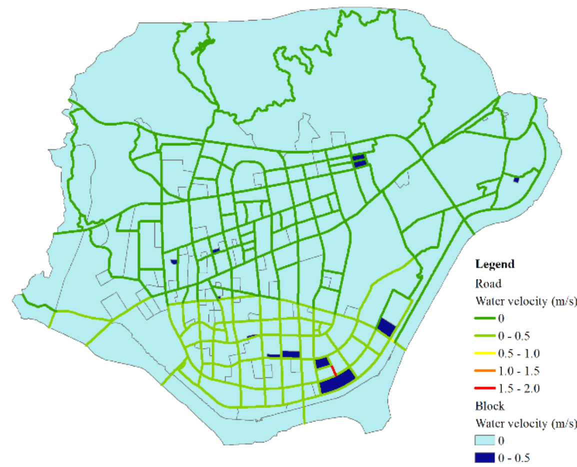

(a) Water depth (pluvial flood, T = 15:00) (b) Water velocity (pluvial flood, T = 08:00)

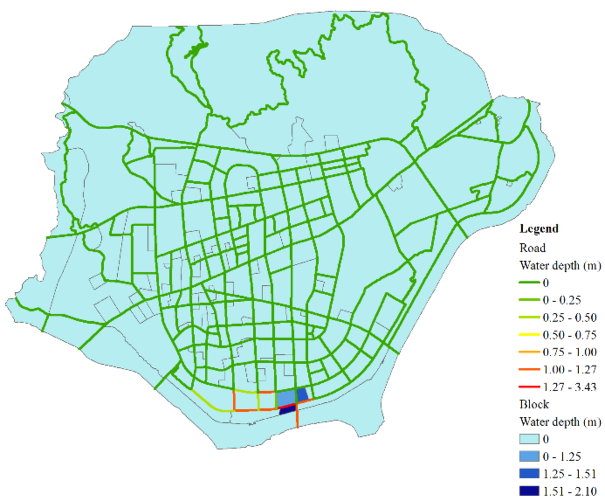

(c) Water depth (fluvial flood, T = 16:00) (d) Water velocity (fluvial flood, T = 16:00)

Figure 9. Accumulated water depths and velocities. T means time here.

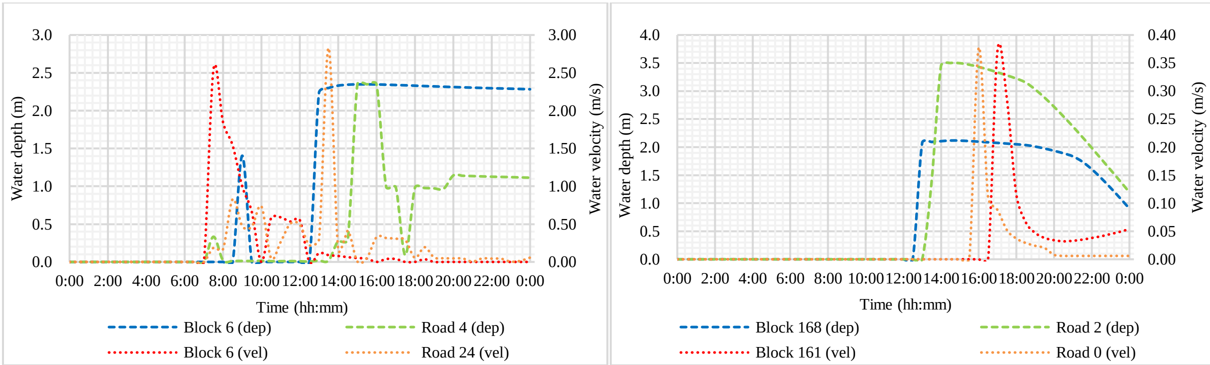

(a) Pluvial flood (b) Fluvial flood

Figure 10. Changes in the surface water depths and velocities for eight severely flooded areas. The “dep” indicates water depth, and “vel” indicates water velocity.

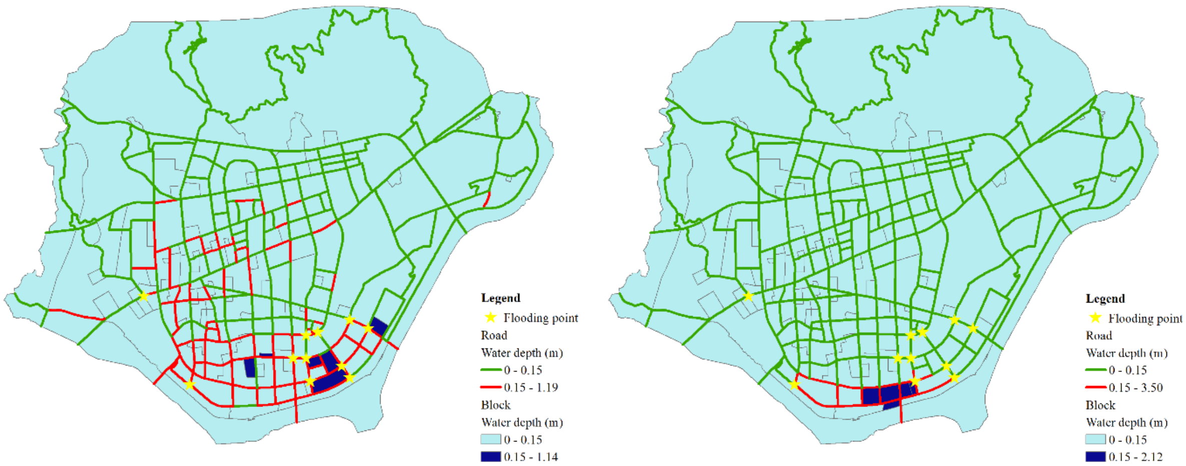

(a) Pluvial flood (b) Fluvial flood

Figure 11~~6~~. Map of the flooded area indicating the flooding simulation and the real flood in 2014. The information for the flooded area was provided by Lishui City Housing and Urban-Rural Construction Bureau.

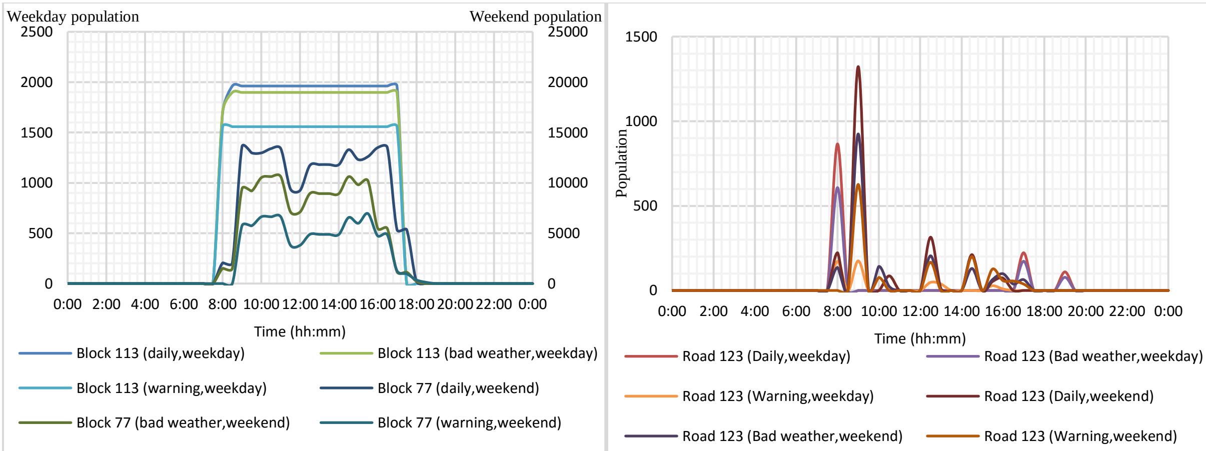

(a) Block (b) Road

Figure ~~11~~12. Population changes in blocks and roads for the six scenarios.

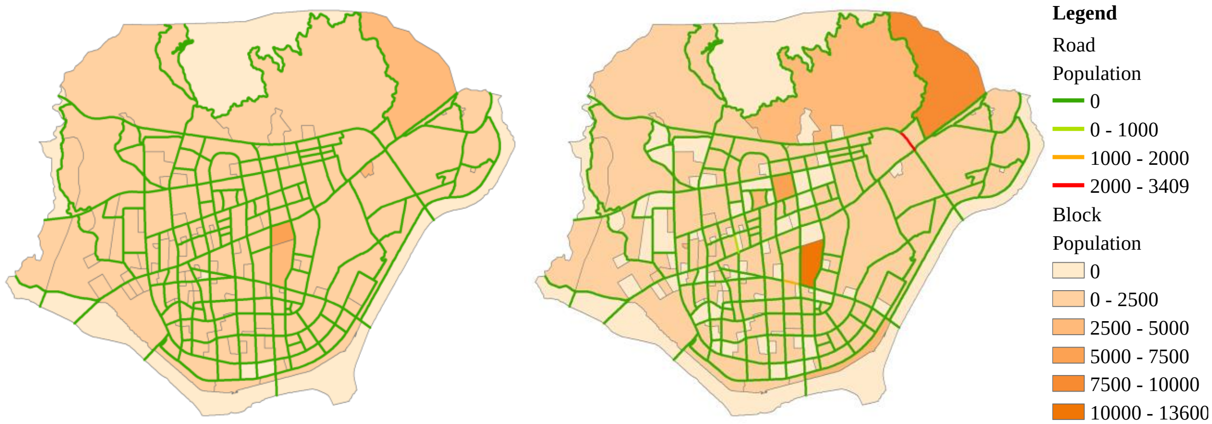

(a) Daily, weekday (T = 09:00) (b) Daily, weekend (T = 09:00)

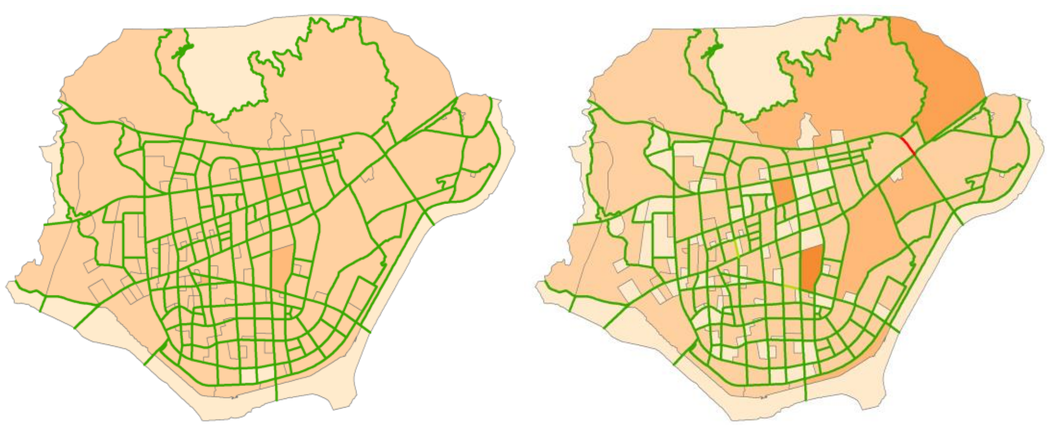

(c) Bad weather, weekday (T = 09:00) (d) Bad weather, weekend (T = 09:00)

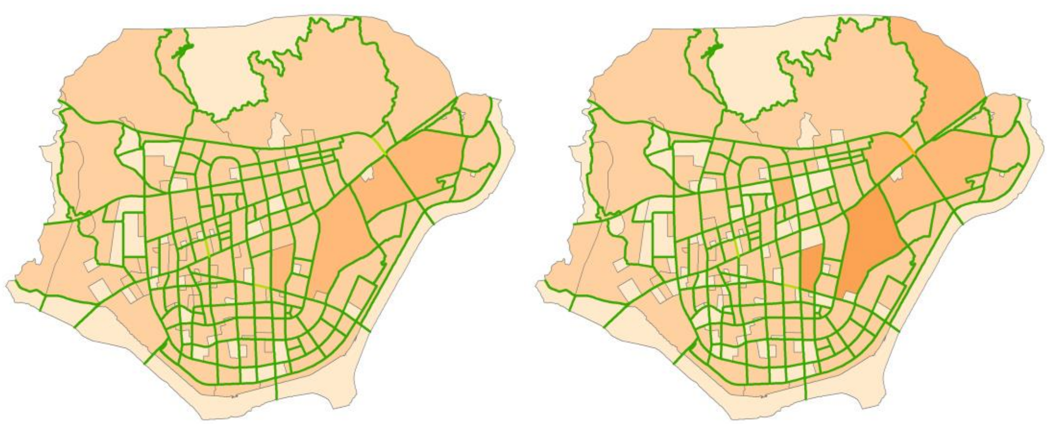

(e) Warning, weekday (T = 09:00) (f) Warning, weekend (T = 09:00)

Figure ~~12~~13. Population distribution for the six scenarios. T means time here.

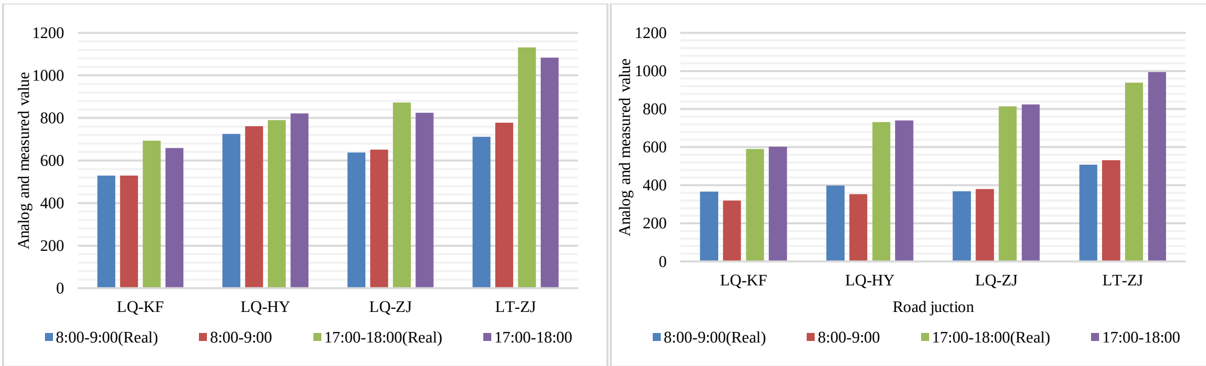

(a) Weekday (b) Weekend

Figure 14. Traffic flow and population simulation results during peak hours on weekdays and weekends. The traffic flow data were provided by the Lishui City Traffic Bureau. Real means measured value here. LQ is Liqing Road, KF is Kaifa Road, HY is Huayuan Road, ZJ is Zijin Road, and LT is Lutang Street.

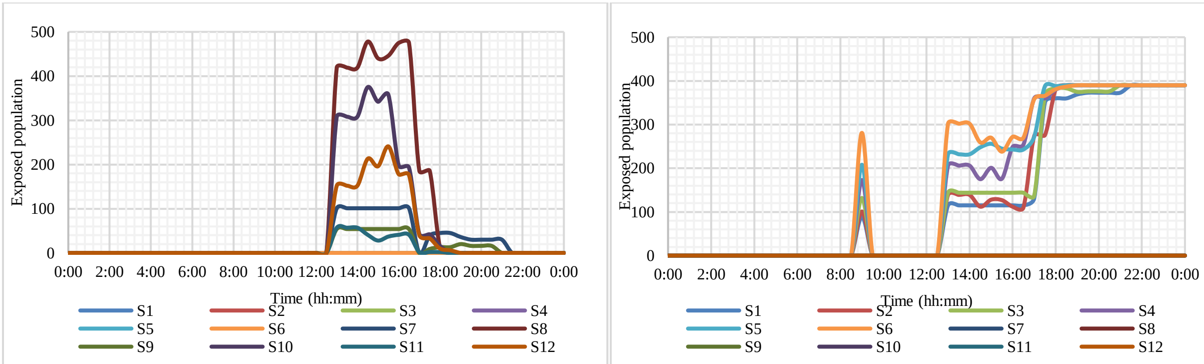

(a) Population exposure (Block 168)

(b) Population exposure (Block 6)

Figure ~~13~~15. Changes in the population exposure of two blocks for the 12 scenarios. Block 168 was a recreational area, and Block 6 was a residential area.

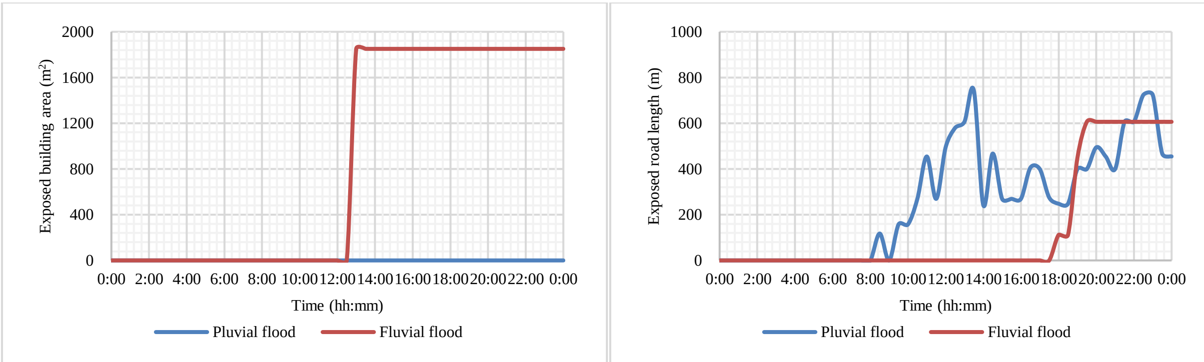

(a) Exposed building area (Block 168) (d) Exposed road length (Block 6)

Figure 146. Changes in road and building exposures in severely flooded blocks. The exposed road length and building area represent road and building exposures, respectively.

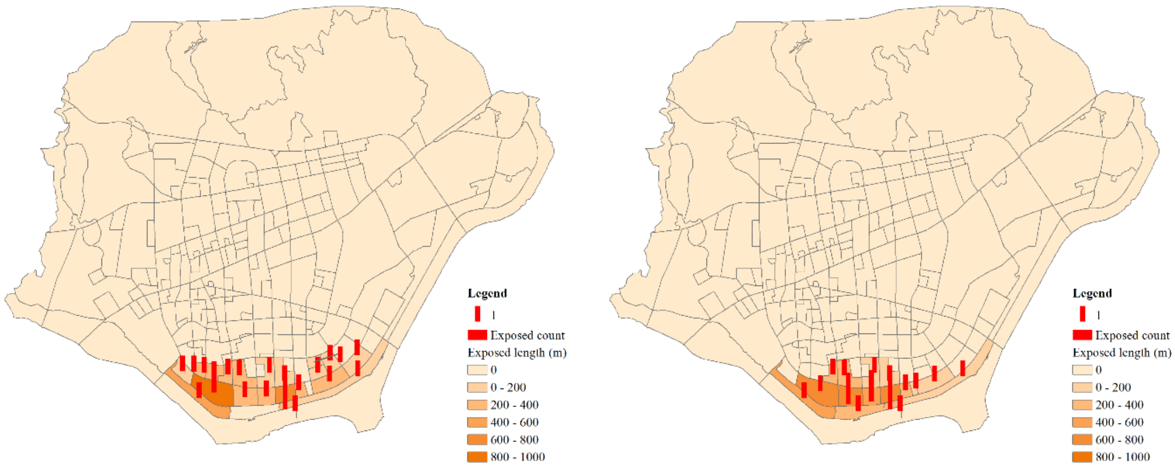

(a) Road exposure (pluvial flood, T = 18:30) (b) Road exposure (fluvial flood, T = 18:30)

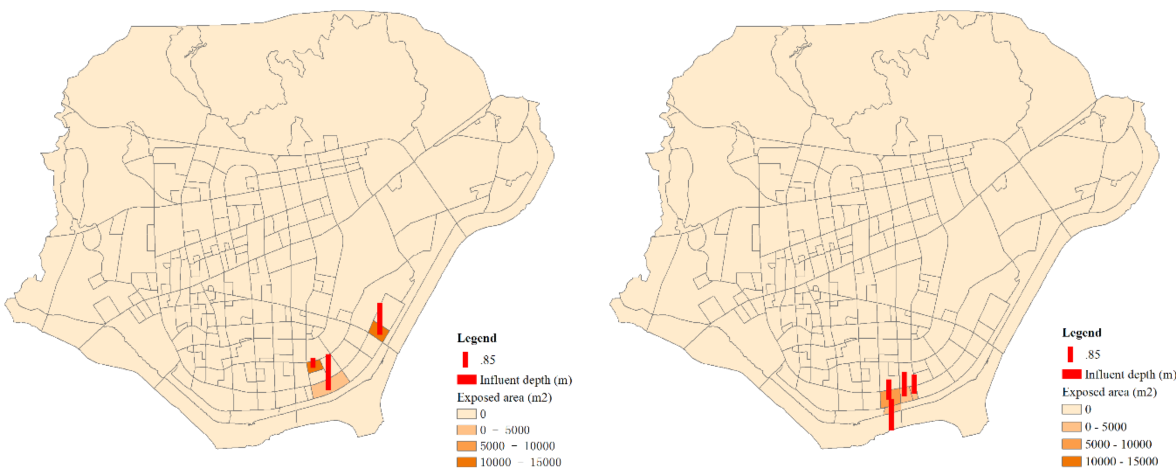

(c) Building exposure (pluvial flood, T = 18:30) (d) Building exposure (fluvial flood, T = 18:30)

Figure 17~~5~~. Map of road and building exposures. T means time here.

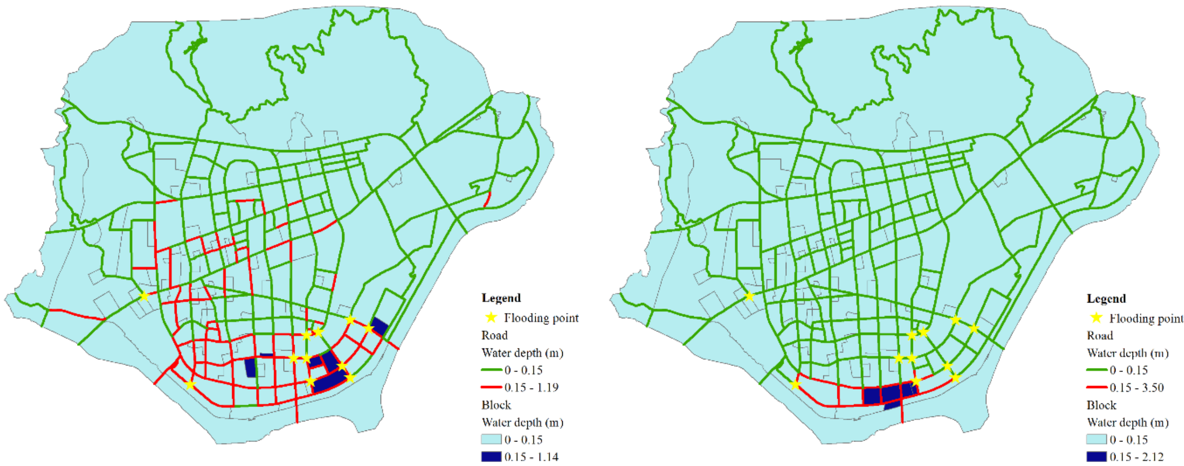

~~(a) Pluvial flood~~ ~~(b) Fluvial flood~~

~~**Figure 16.** Map of the flooded area indicating the flooding simulation and the real flood in 2014. The information for the flooded area was provided by Lishui City Housing and Urban-Rural Construction Bureau.~~

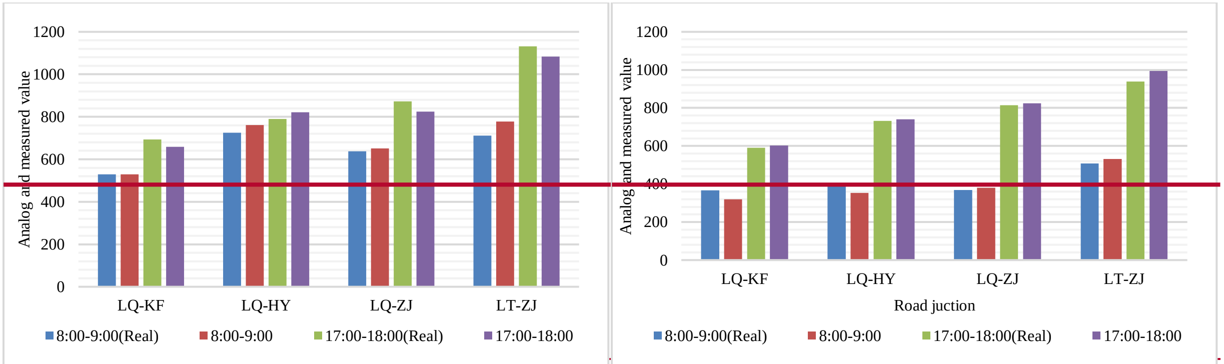

~~(a) Weekday~~ ~~(b) Weekend~~

~~**Figure 17.** Traffic flow and population simulation results during peak hours on weekdays and weekends. The traffic flow data were provided by the Lishui City Traffic Bureau. Real means measured value here. LQ is Liqing Road, KF is Kaifa Road, HY is Huayuan Road, ZJ is Zijin Road, and LT is Lutang Street.~~

Table 1 Data used in this study.

Table 2. Parameter values for the rainstorm intensity formula.

Table 3. Parameter variations used in the simulation scenarios.

Table 4. Sociodemographic characteristics of the population in the case study area.

Table 5. Building step heights for different block types.

Table 1. Data used in this study.

Data	Source	Time	Use
Digital elevation model	Local government	2013	Topography
Basic geographic data	Local government	2015	Location of river, road and building
Hydrological data	Local government	20 Aug 2014	Flow and water level
1km grid population data	National Earth System Science Data Sharing Infrastructure, National Science & Technology Infrastructure of China (http://www.geodata.cn)	2010	Number of residents in grid of the study area.
Population profile	Lishui Statistical Yearbook and Liandu Yearbook (http://tjj.lishui.gov.cn/sjjw/tjnj/201511/t20151105_448284.htm)	2014	Gender profile, age profile, education level profile, employment profile and travel mode profile were used to classify agent groups.
Traffic flow data	Local government	24 June 2017 to 7 July 2017	The number of vehicles passing through a node within one hour at four intersections from 24 June 2017 to 7 July 2017 in this area,
Water accumulation point	Local government (http://www.zjjs.com.cn/n17/n26/n44/n47/c339697/content.html)	20 Aug 2014	Location

Table 2. Parameter values for the rainstorm intensity formula.

Parameter	Value
A	1265.3
b	5.919
c	0.587
n	0.611

Table 3. Parameter variations used in the simulation scenarios.

Scenarios	Flooding Type	Human behavior	Weekdays or Weekends
S1	Pluvial flood	Daily	Weekdays
S2	Pluvial flood	Daily	Weekends
S3	Pluvial flood	Bad weather	Weekdays
S4	Pluvial flood	Bad weather	Weekends
S5	Pluvial flood	Warning	Weekdays
S6	Pluvial flood	Warning	Weekends
S7	Fluvial flood	Daily	Weekdays
S8	Fluvial flood	Daily	Weekends
S9	Fluvial flood	Bad weather	Weekdays
S10	Fluvial flood	Bad weather	Weekends
S11	Fluvial flood	Warning	Weekdays
S12	Fluvial flood	Warning	Weekends

Table 4. Sociodemographic characteristics of the population in the case study area.

Variables	Groups	Percentage (%)
Gender	Male	50.430
	Female	49.570
Age	0-17	18.730
	18-60	63.340
	>60	17.930
Professional status	Employed	55.770
	Unemployed	44.230
Education Level	University, school-college, bachelor	14.457
(Highest diploma)	No diploma	85.543
Travel mode	Walk	25.24
	Bus	43.06
	Car	31.70

Note: The data are from the 2015 Lishui Statistical Yearbook and 2015 Liandu Yearbook.

Table 5. Building step heights for different block types.

No	Block type	Building type	Building steps height
1	Residential area I	Garden house, villa	0.35 m（floors>9, 0.60 m）
2	Residential area II	High-rise apartments and new village houses before and after liberation (before 1988); new residential quarters and commercial houses (after 1988)	0.35 m（floors>9, 0.60 m）
3	Residential area III	New and old Lane homes, three types of staff housing	0.10 m
4	Residential area IV	Shed house	0.05 m
5	School	Educational building	0.35 m（floors>9, 0.60 m）
6	Company	Office building	0.35 m（floors>9, 0.60 m）
7	Recreational area	Public buildings for business, culture, sports and other use	0.35 m（floors>9, 0.60 m）